Journal of Membrane Science & Research

journal homepage: www.msrjournal.com

Research Paper

Experimental Design for Nano-Ceramic Membranes Fabrication and Optimization

Heba Abdallah [1], Ayman El–Gendi [1,*], Ahmed Mohamed Ismail [2], Ashraf Amin [1], Shereen Kamel Amin [1]

[1] *Chemical Engineering and Pilot Plant Department, Engineering and Renewable Energy Research Institute, National Research Centre (NRC), Giza, Egypt, Affiliation ID: 60014618*
[2] *Industrial Technological Development Sector – Ministry of Investment, Trade, and Industry, Cairo, Egypt*

Article info

Received 2021-10-22
Revised 2022-02-09
Accepted 2022-02-11
Available online 2022-02-11

Keywords

Nano-ceramic membrane
Desalination
Experimental design
Optimization

Highlights

- Nano-ceramic membranes were fabricated using waste powder produced from ceramic industries.
- The Experimental model design for ceramic membranes fabrication was studied using the factorial design method.
- A mathematical model was developed to predict the properties of the produced membranes.
- A mathematical model was developed to predict the performance of the prepared membranes for water desalination.
- The predicted salt rejection of the model was matched with the experimental results, which reached 99.8%.

Graphical abstract

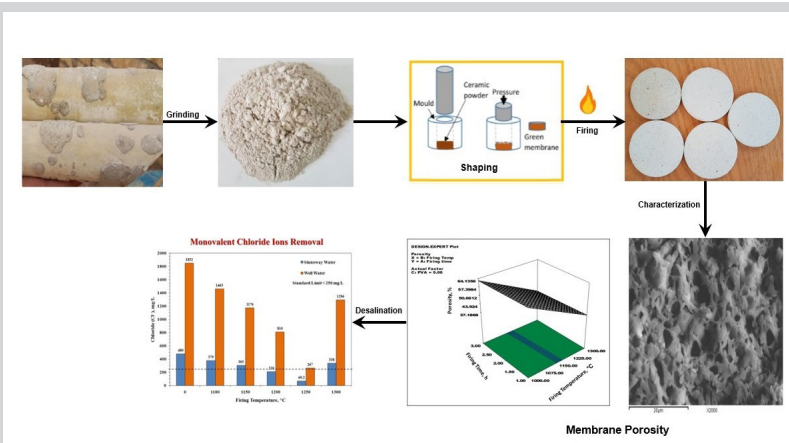

Abstract

In this work, nano-ceramic membranes were fabricated using waste powder produced from ceramic industries. An experimental model for fabricating ceramic membranes for desalination was developed using the factorial design method. The (33) factorial designs (FD) were employed to study the effect of verification parameters, such as time, binder percentage, and firing temperature on the prepared membrane properties, including bulk density, apparent specific gravity, apparent porosity, and water absorption. The three-dimensional (3D) response surface plot FD model of water absorption using 5% polyvinyl alcohol (PVA) indicated that increasing firing temperature resulted in a reduction in membrane water absorption and porosity. The maximum achievable porosity was 47–48%, observed at a firing temperature of 1200°C. The minimum porosity was 33%, observed at a firing temperature of 1300°C. A mathematical model was developed for optimizing the membrane for desalination using different salt concentrations ranging from 5 to 45 g/L. The model predictions indicate that the water permeate flux is decreased as the feed salt concentration increases as observed from the experimental results. The predicted salt rejection from the model agreed with the experimental results, it was around 99.8–99.6% reduction of the feed salt concentration.

1. Introduction

A ceramic membrane is a separation tool formed from inorganic ceramic materials (zirconia, alumina, titania, and others) [1–5]. Ceramic membrane usually consists of multiple layers of ceramic materials [1,2]. Ceramic membranes and their applications are controlled by the pore size of the membrane [6–9]. Macroporous membranes have a pore size of > 50 nm. While mesoporous membranes have smaller pore sizes of 2 to 50 nm. Finally, microporous membranes have pore sizes < 2 nm, and dense membranes contain no pores [10–16]. In general, suspended matter and bacteria are separated easily by microfiltration (MF) membranes [3] although MF membranes fail to eliminate some dissolved matter and certain microorganisms [17–24]. Therefore, membranes with smaller pore sizes, such as nanofiltration or reverse osmosis (RO) membranes, are suitable for separating viruses and dissolved materials in seawater [4, 5].

In the last two decades, the significance of ceramic membranes is proven in several applications, such as water desalination [25–29]. Generally, ceramic membranes prepared from raw, low-cost material is a smart option for further development in the water treatment field [6, 30]. Desalination of seawater by the ceramic membrane is one of the favorable choices [7, 8].

* Corresponding author: aymantaha2010@yahoo.com (A. El–Gendi)

DOI: 10.22079/JMSR.2022.539537.1497

Several membrane models described in the literature have been proposed to simulate the performance of ceramic membranes [9, 10]. Mathematical models are an essential tool for studying the performance of several membranes and estimating the performance of the membrane under variable operating conditions [10–15]. Two model categories are applied in the literature: (1) lumped parameter model and (2) mechanistic model (membrane transport model) [9].

The mechanistic model assumes that the thin top skin of asymmetric membranes or composite membranes is at equilibrium during the membrane diffusion process [10]. The mechanistic model can be further divided into a nonporous or homogenous membrane, irreversible thermodynamics, and pore models [11, 12]. The nonporous model category assumes that the membrane is nonporous and diffusion is the mechanism by which ion transport occurs. The pore model presumes that ion transport occurs via the membrane barrier layer. The lamped parameter models are more appropriate for developing a model for control applications operating under transient state conditions or when the membrane is operating at a steady-state [13–18]. The nonporous model's category includes different models similar to the solution-diffusion models. The solution-diffusion models presume that both solvent and solute are diffusing through the membrane [30, 31].

The solution-diffusion model was developed assuming diffusion of both solvent and solute, and five assumptions should be considered while using such a model [14, 32]. This category of models can be applied for organic and inorganic solutes especially for low water content membranes due to the poor prediction of the water flux [15, 33]. The solution-diffusion models do not take into account the effect of membrane layer defects and imperfections and do not explain the solute rejection [16, 34].

To overcome the solution-diffusion models' limitations, Sourirajan [17] established the pore-diffusion model, assuming that the membrane has a micro-porous structure. The viscous flow through uniform membrane pores is dominated by the solvent transportation mechanism. The membrane barrier layer repels solutes and absorbs solvents. Solute transport occurs as a result of diffusion and convection. However, Alexiadis et al. [18] observed that the effect of operating pressure may lead to a remarkable error in the pore-diffusion model. Alexiadis et al. [18] determined that inconsistency between experimental lab results and the model increased as the operating pressure increased, which is attributed to the effects of pressure on membrane structure that may lead to membrane compaction. A better agreement between the model and the experimental results can be achieved by optimizing the model parameters despite the operating pressure value.

The factorial design of experiments can be used to ensure an experimental study that is conclusive for the factors under consideration [13–18]. Using the factorial design will enable data processing with the aim of developing mathematical relationships between the dependent and the process parameters. The factorial design was used in our study to develop a mathematical relationship between the different parameters considered during membrane production. These relationships can provide a valuable understanding of the effects of each parameter [19].

A mathematical model was used to study ceramic membrane manufacturing [9, 14]. The experimental work was conducted according to the factorial design of experiments, and the experimental results were used to develop a mathematical model [15–18]. In this work, factorial design software was used for experimental design to determine the optimum fabrication conditions for nano-ceramic membranes that were prepared from waste powder generated in the ceramic industries. Additionally, the mathematical model for the membrane performance was investigated to compare the experimental results with predicted results from the model.

2. Methods and Experimental Work

2.1. Experimental model design for ceramic membranes fabrication using factorial design

A (3^3) factorial design (FD) was used to study the effect of verification parameters on the prepared membrane properties, including apparent porosity, apparent specific gravity, water absorption, and density [20, 21]. The independent parameters were varied at three different levels. Four properties of the produced ceramic membranes were measured as a response to the variation of the independent parameters. A full factorial design was developed by considering several parameters: (1) firing time (t), (2) polyvinyl alcohol (PVA) concentration, and (3) firing temperature (T). The parameters values under study and the detailed experimental plan are shown in Table 1.

Each property value of the developed membrane can be calculated using a four terms polynomial as a function of firing time, PVA concentration, and firing temperature (Equations 1–4). Using the least-square methods, the model parameters were fitted by minimizing the error between the model predictions and the experimental data. Equations 1–4 coefficients were fitted by comparing the experimental results with the equations' prediction. By changing the values of the coefficients to minimize the square error of the discrepancy between lab-observed values and model prediction, the optimum coefficients' values could be determined. The least-square method was used to approach the optimum fitting by minimizing the sum of the residual sum of squares for each equation [22, 23]. The resulting equations and statistical analysis for each equation are shown below:

The water absorption (WA) of the prepared ceramic membrane can be calculated from Equation (1).

$$\text{Water Absorption (WA, \%)} = 142.4 - 0.425\ t - 0.4124\ PVA - 0.092\ T \quad (1)$$

where t is the firing time (h), PVA is the PVA Concentration (%), and T is the temperature (°C).

The apparent porosity (P) of the prepared ceramic membrane can be calculated from Equation (2).

$$\text{Apparent Porosity (P, \%)} = 151.84 - 0.8144\ t - 0.33\ PVC - 0.0844\ T \quad (2)$$

The bulk density (BD) of the prepared ceramic membrane can be calculated from Equation (3).

$$\text{Bulk Density (BD, g/cm}^3\text{)} = -2.75 + 0.00185\ t + 0.0164\ PVC + 0.00357\ T \quad (3)$$

The apparent specific gravity (SG) of the prepared ceramic membrane can be calculated from Equation (4).

$$\text{Specific Gravity (SG)} = 1.155 - 0.037\ t + 0.00715\ PVC + 0.00162\ T \quad (4)$$

2.2. Membrane performance mathematical model

The ceramic membrane can be applied in water treatment and desalination [24, 25]. The mathematical model for the dead-end mode desalination test was investigated and established according to a set of experimental data collected in our lab [26, 27].

This model was developed to study reverse osmosis (RO) in the ceramic membrane. The model assumptions and equations are shown below:

- The RO membrane structure is nonporous, and the surface layer is homogenous.
- The solvent dissolves in and diffuses through the surface layer.
- The diffusion of the solvent and solute are uncoupled, which is attributed to the existence of a chemical potential gradient through the membrane.
- The chemical potential gradient is a function of pressure difference through the membrane and concentration.
- The solution on the two membranes sides is homogenous, and the solute is uniformly mixed, so no active diffusion takes place within one side.

Fick's law can be used to calculate the diffusion of the solvent (J_w) [28]:

$$J_W = -D_{Wm}\frac{dC_{Wm}}{dz} \quad (5)$$

where, D_{Wm} is the solvent diffusivity (water diffusivity: 3E-8 m^2/s) and C_{Wm} is the solvent concentration through the membrane is a function of the solvent's (water) chemical potential (μ_W).

Osmotic pressure (π) can be determined from the following equation [10]:

$$\pi = \phi\left(\frac{n}{v}\right) R_g T \quad (6)$$

where, $\emptyset$ is the seawater osmotic pressure coefficient ($\emptyset = 2$), n is the dissolved solute number of moles v is the volume of the mixer, R_g is the universal gas constant (0.00831 L.bar/kmol) and T is the temperature.

The rejection ratio (R) can be determined from the following Equation:

$$R(\%) = (1 - \frac{C_P}{C_f}) \times 100 \quad (7)$$

where, C_P is the permeate sides solute concentration, and C_f is the feed side solute concentration.

Finally, the water and solute fluxes can be calculated using the following Equations respectively [10]:

$$N_w = A(\Delta P - \Delta\pi) + K_1 * \Delta P \quad (8)$$

$$N_s = B(C_f - C_P) + K_2 * \Delta P \quad (9)$$

where, A and B are two parameters used to characterize the system, K_1 and K_2 are experimentally fitted parameters, and ΔP is the pressure difference across the membrane.

Table 1
A (3^3) factorial design for verification parameters.

Number	Time (t), h			PVA Concentration, %			Temperature (T), °C		
	-	*	+	-	*	+	-	*	+
	1	2	3	3	4	5	1200	1250	1300
	Coded units for factors			The average response from duplicate runs					
	t	PVA	T	Bulk Density (g/cm^3)	Apparent Porosity (%)		Water Absorption (%)	Apparent Specific Gravity	
1	-	-	-	1.614	44.98		27.86	2.93	
2	-	-	*	1.64	46.54		28.32	3.07	
3	-	-	+	1.92	39.74		20.69	3.18	
4	-	*	-	1.671	45.96		27.49	3.09	
5	-	*	*	1.72	46.56		26.94	3.23	
6	-	*	+	1.96	38.27		19.44	3.19	
7	-	+	-	1.63	46.66		28.47	3.07	
8	-	+	*	1.67	45.78		27.29	3.09	
9	-	+	+	2.05	42.04		20.50	3.53	
10	*	-	-	1.64	48.39		29.50	3.18	
11	*	-	*	1.69	46.42		27.34	3.16	
12	*	-	+	1.90	36.16		19.01	2.97	
13	*	*	-	1.66	44.85		26.96	3.01	
14	*	*	*	1.69	46.30		27.31	3.15	
15	*	*	+	2.11	38.41		18.18	3.43	
16	*	+	-	1.65	44.72		27.00	2.99	
17	*	+	*	1.69	46.57		27.49	3.17	
18	*	+	+	2.09	39.66		18.91	3.47	
19	+	-	-	1.60	48.31		30.12	3.10	
20	+	-	*	1.70	49.17		28.79	3.36	
21	+	-	+	1.98	33.83		17.05	2.99	
22	+	*	-	1.69	47.10		27.76	3.20	
23	+	*	*	1.69	43.95		25.94	3.02	
24	+	*	+	2.06	37.34		18.08	3.29	
25	+	+	-	1.65	45.60		27.61	3.03	
26	+	+	*	1.59	41.41		25.96	2.72	
27	+	+	+	1.948	35.14		18.04	3.00	

3. Results and Discussions

3.1. Water absorption

The water absorption of the prepared ceramic membrane results predicted by factorial design software and compared to results from this experimental work [21–28] indicated good matching as shown in Fig. 1.

Fig. 1 shows the parity plot as a comparison between experimental and calculated (Equation 1) water absorption of the prepared membrane. Fig. 1 indicates that Equation 1 can predict the ceramic membrane water absorption under different preparation conditions, including time, PVA%, and firing temperatures.

The prepared samples were fired at different conditions by varying the soaking time, PVA%, and temperatures. The results indicated that water

absorption increases with increasing the firing temperature up to 1200°C, which is attributed to the increased membrane porosity. Increasing the temperature further, sintering plays a role in leading to lower porosity as indicated by water absorption decrease. PVA is expected to decompose below 500°C which explains the limited effect of PVA% on the porosity. The results indicated that firing temperature is the dominant factor in water absorption. Soaking for more than one hour did not have any effect on water absorption.

On the other hand, the regression analysis and analysis of variance (ANOVA) for parameter fittings and statistics for Equation 1 are presented in Tables 2 and 3, respectively. From these tables, the statistical analysis shows a reasonable R^2 and a reasonable F value that is much higher than the significant F value, which confirms that Equation 1 can be used for calculating water absorption within the experimental range in this study [29].

The FD model solution of membrane water absorption as a function of firing time and firing temperature at 5% PVA (as an example) is presented in Fig. 2. The model shows the contour graph (a) and (b) the 3D response surface plot model solution of water absorption using 5% PVA. To avoid redundancy, figures corresponding to PVA concentrations of 2% and 3% were not reported since their results were very similar to those previously mentioned. The model results indicated that increasing firing temperature may lead to a decrease in membrane water absorption. Temperature is the key parameter for inducing the amount of water absorption. That finding agrees with the experimental results in which water absorption increased up to about 1200°C. While a further increase in temperature may lead to a drop in water absorption.

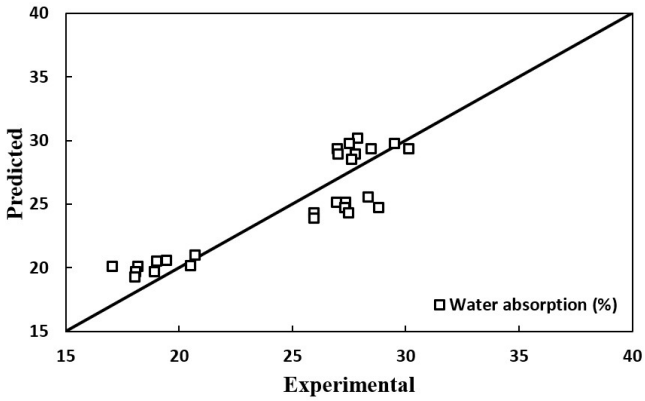

Fig. 1. Experimental and predicted water absorption.

Table 2
Regression analysis for Equation (1).

Regression Analysis	
Multiple R	0.88
R Square	0.78
Adjusted R Square	0.75
Standard Error	2.16
Observations	27

Table 3
ANOVA table for parameters fitting and statistics of Equation (1).

	df	SS	MS	F	Significance F
Regression	3	388.20	129.40	27.68	8.21E-08
Residual	23	107.50	4.67		
Total	26	495.71			

3.2. Apparent porosity

The predicted apparent porosity of the ceramic membrane using Equation 2 agrees well with the experimental work, as shown in Fig. 3.

Fig. 3 shows a comparison between experimental and predicted apparent porosity of the prepared membrane using Equation 2. Fig. 3 indicates that Equation 2 can predict the membrane apparent porosity under different preparation conditions, including time, PVA%, and firing temperature.

The effect of temperature, soaking time, and PVA% showed on the apparent porosity a trend similar to that observed with water absorption. The maximum porosity was 47-48%, observed at a firing temperature of 1200°C. The minimum porosity was 33%, observed at a firing temperature of 1300°C and a soaking time of 3 h. The results indicated that soaking time has less effect on the apparent porosity compared to the firing temperature as observed with the water absorption.

Alternatively, Tables 4 and 5 display the regression analysis and ANOVA for parameter fitting and statistics for Equation 2, respectively. From these tables, the statistical analysis shows an R^2 of 0.65 and an F value of 14.65 compared to a significant F value of 1.57^{-5}, confirming that Equation 2 can be used for calculating apparent porosity within the experimental range under study.

Also, the FD model solution of membrane porosity as a function of firing time and firing temperature at 5% PVA (as an example) is presented in Fig. 4. The model shows the contour graph (a) and (b) 3D response surface plot model solution of membrane porosity using 5% PVA. To avoid redundancy, results with PVA concentrations of 3% and 4% were not reported. However, a trend similar to those previously mentioned with 5% PVA was observed at both of these concentrations. The model results indicate that increasing firing temperature caused a reduction in porosity, similar to the experimental results indicating a good agreement between the model prediction and the experimental results.

3.3. Bulk density

Fig. 5 shows the bulk density of the prepared ceramic membrane results that were predicted by the factorial design software model and compared with results from experimental work for the parity plot, which indicated good matching. The two plots indicate that Equation 3 could be used to foresee the ceramic membrane bulk density under different preparation conditions, including firing time, PVA concentration, and firing temperature.

The bulk density of the membrane is a function of the total porosity of the body and the membrane's true density. The true density does not change significantly during firing. The membrane porosity is inversely proportional to the bulk density. The firing temperature is the dominant factor in the bulk density. The maximum bulk density was 2.05 g/cm^3, observed at 1300°C. The experimental results indicated that soaking time and PVA% do not affect the bulk density.

Otherwise, Tables 6 and 7 present the regression analysis and ANOVA for parameter fitting and statistics for Equation 3. From these tables, the statistical analysis yielded 0.75 for R^2 and 23.38 for F value compared to a significant F value of 3.59^{-5}, a finding that confirms that Equation 3 can be used correctly for calculating apparent porosity within the experimental range under study.

Furthermore, the FD model solution of membrane bulk density as a function of soaking time and firing temperature at 5% PVA (as an example) is presented in Fig. 6. It illustrates the contour graph (a) and (b) 3D response surface plot model solution of membrane bulk density using 5% PVA. The model results indicate that increases in firing temperature led to an increase in bulk density. Our experimental results also indicated bulk density reached a maximum value of 2.05 g/cm^3 at a firing temperature of 1300°C.

3.4. Apparent specific gravity

The apparent specific gravity of the ceramic membrane as predicted by Equation 4 agrees with the experimental results, as shown in Fig. 7 that indicates that Equation 4 can predict the ceramic membrane's apparent specific gravity under different preparation conditions, including different PVA%s, firing times, and temperatures.

The firing temperature was found to have the largest effect on the membrane-specific gravity. Also, the binder concentration does not affect the membrane-specific gravity, while the soaking time has a minimum effect.

Moreover, the regression analysis and ANOVA for parameter fittings and statistics for Equation 4 are presented in both Tables 8 and 9, respectively. From these tables, the statistical analysis yielded an R^2 of 0.17 and an F value of 1.66 compared to a significance F value of 0.2, which confirms that Equation 4 can be used for calculating apparent specific gravity value as an indication within the experimental range understudy with low precision.

Also, Fig. 8 shows the FD model solution of membrane-specific gravity as a function of firing time and firing temperature at 5% PVA (as an example). The figure illustrates the contour graph (a) and (b) 3D response surface plot model solution of membrane specific gravity at PVA 5%. The model results indicate that increasing the firing temperature caused an increase in specific gravity.

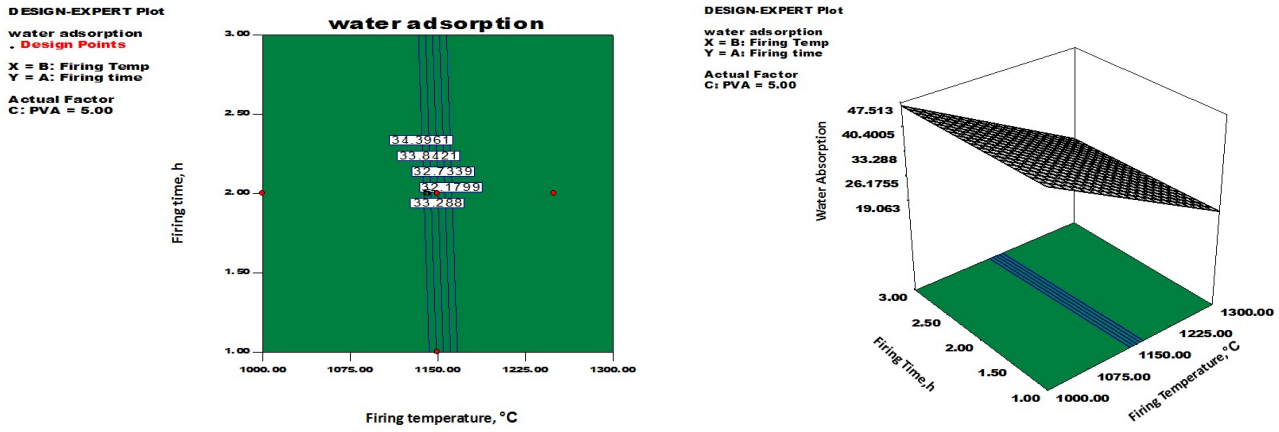

(a) **(b)**

Fig. 2. FD model solution of membrane water absorption as a function of firing time and firing temperature at 5% PVA, where: (a) contour graph; and (b) three-dimension response surface plot.

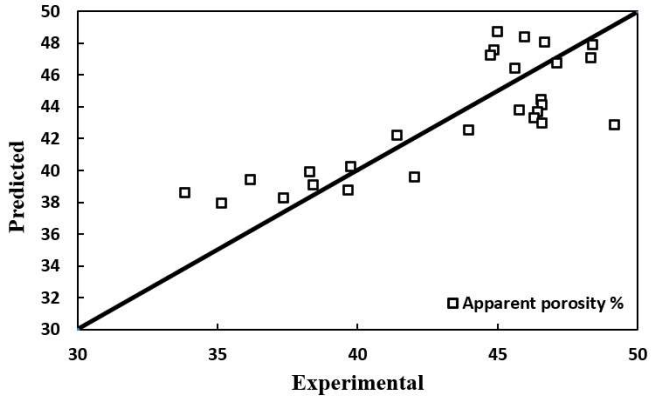

Fig. 3. Experimental and predicted apparent porosity.

Table 4
Regression analysis for Equation (2)

Regression Analysis	
Multiple R	0.81
R Square	0.65
Adjusted R Square	0.61
Standard Error	2.76
Observations	27

Table 5
ANOVA table for parameters fitting and statistics of Equation (2).

	df	SS	MS	F	Significance F
Regression	3	334.82	111.60	14.56	1.57E-05
Residual	23	176.29	7.66		
Total	26	511.12			

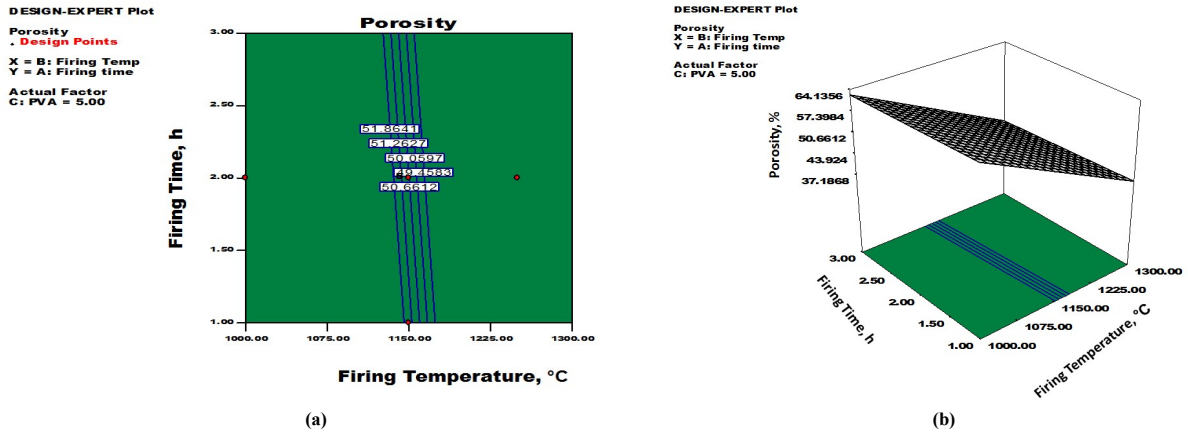

(a) (b)

Fig. 4. FD model solution of membrane porosity as a function of firing time and firing temperature at 5% PVA, where: (a) Contour graph; and (b) Three-dimension response surface plot

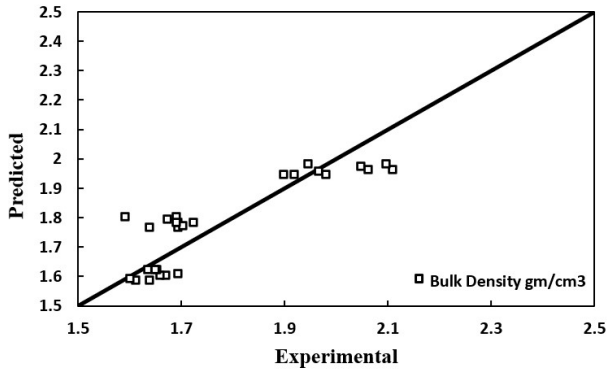

Fig. 5. A parity plot for the experimental and calculated bulk density.

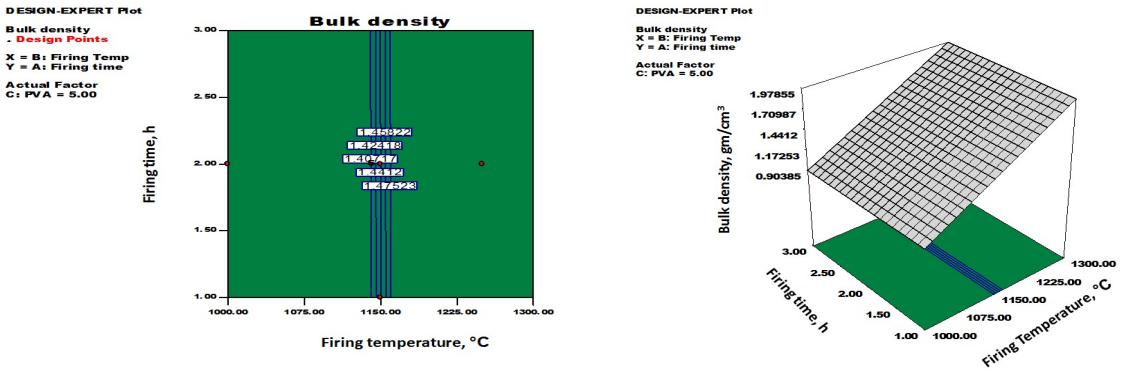

(a) (b)

Fig. 6. FD model solution of membrane bulk density as a function of soaking time and firing temperature at 5% PVA, where (a) Contour graph; and (b) Three-dimension response surface plot.

Table 6

Regression analysis for Equation (3).

Regression Analysis	
Multiple R	0.86
R Square	0.75
Adjusted R Square	0.72
Standard Error	0.09
Observations	27

Table 7

ANOVA table for parameters fitting and statistics of Equation (3).

	df	SS	MS	F	Significance F
Regression	3	0.57	0.19	23.38	3.59E-07
Residual	23	0.19	0.01		
Total	26	0.76			

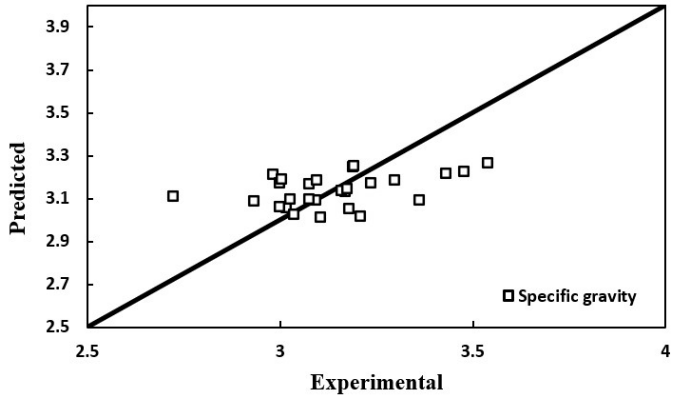

Fig. 7. A parity plot for the experimental and calculated apparent specific gravity

Table 8

Regression analysis for Equation (4).

Regression Analysis	
Multiple R	0.42
R Square	0.17
Adjusted R Square	0.07
Standard Error	0.16
Observations	27

Table 9

ANOVA table for parameters fitting and statistics of Equation (4).

	df	SS	MS	F	Significance F
Regression	3	0.14	0.04	1.66	0.20
Residual	23	0.66	0.02		
Total	26	0.80			

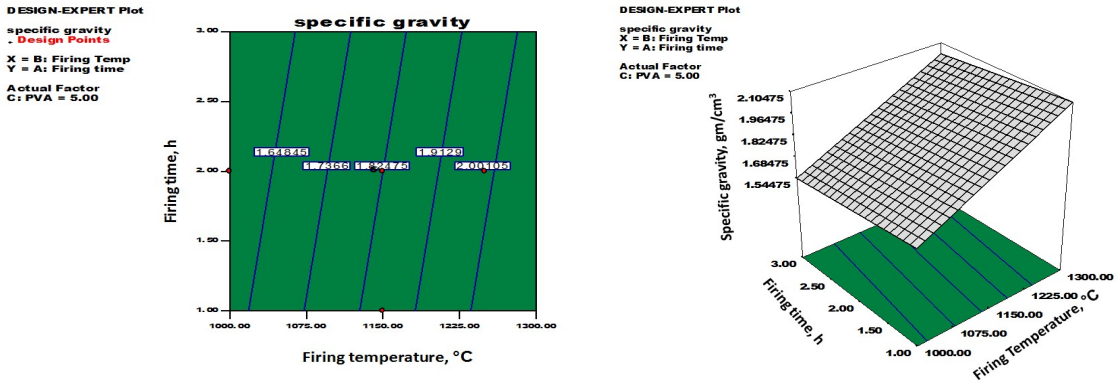

(a) **(b)**

Fig. 8. FD model solution of membrane specific gravity as a function of firing time and firing temperature at 5% PVA, where (a) Contour graph; and (b) Three-dimension response surface plot.

3.5. Mathematical model

In the following section, a statistical analysis was performed over the model, and experimental results for water flux, salt flux, and salt rejection are described [27, 28]. Figs 9–11 show a comparison between experimental and predicted water flux, salt flux, and rejection results, respectively. As indicated by the membrane performance in our lab, the optimum performance of the ceramic membrane could be observed under preparation conditions of 3% PVA and firing at a temperature of 1250 ºC for 1 h soaking time. The proposed model was developed and fitted according to the experimental data collected using the best performance ceramic membrane [13–18]. The least-squares method fitting was used to estimate the parameters for predicting water absorption, rejection ratio, and salt fluxes. Recalling Equations 8 and 9, the parameters were estimated using the least-square method. The parameters are shown in Table 10. The model could be verified by comparing its predictions with the experimental data. A good agreement was observed as shown in Figs 9–11, respectively.

The water flux of the ceramic membrane, which was prepared under optimum conditions, was predicted by Equation 8. Using parameters in Table 10, Equation 8 yielded excellent predictions as indicated by the R^2 value of 0.95. Comparing the observed F and significance F values (57.6 and 0.0047, respectively), Equation 8 represents a good fit for experimental data as confirmed by Fig. 9, which displays a comparison between experimental and predicted water flux results, in which typical values could be observed.

On the other hand, Equation 9 can be used to calculate the salt flux using the ceramic membrane prepared under optimum conditions. Using parameters

in Table 10, Equation 9 yielded excellent predictions as indicated by an R^2 value of 0.99. Comparing the observed F and significant F values (646 and 0.00013, respectively), Equation 5 fits well with the experimental results as confirmed by Fig. 10, which shows the comparison between experimental and predicted salt flux results for which typical values have been observed.

Also, Fig. 11 shows a comparison between the experimentally reported and the calculated rejection ratios. A reasonable prediction is observed in Fig. 11. The desalination model indicates the prepared ceramic membranes can be used in desalination, different experiments for different salt concentrations were studied.

4. Conclusion

Factorial design is employed to study the effect of verification parameters (binder PVA concentrations, firing temperatures, and firing [soaking] time) on the properties of the fabricated ceramic membrane, including water absorption, apparent specific gravity, bulk density, and apparent porosity. The developed model showed a reasonable agreement with the experimental data as indicated by the statistical tools, such as the significant F, while the coefficient of determination was not high enough to suggest excellent fitting for the data. The A factorial design model indicated that the firing temperature was the only affected parameter. Soaking time and PVA concentrations did not affect the physical properties of the fabricated ceramic membrane. The optimum condition for fabricating the ceramic membrane was found to be 3% PVA and firing at a temperature of 1250 ºC for 1 h soaking time.

The mathematical model was developed to study ceramic membranes for desalination processes. The model equations were fitted using the experimental results. Different desalination experiments using different salty solution concentrations were studied. The firing temperature was shown to play a major role in the membrane characterization and performance. The optimum firing temperature was 1250°C. For the membrane prepared at 1250°C, a salt separation of 99.6-99.8% is achieved using a flux of 244.5 $L/m^2.h$ in a 5000 ppm salty solution concentration or 101.9 $L/m^2.h$ at 45,000 ppm.

Table 10
Estimated values of parameters in Equation (8).

Parameters as listed in Equations (8 & 9)	Value
A	2.45
B	2.94E-7
K1	179.93
K2	9E-4

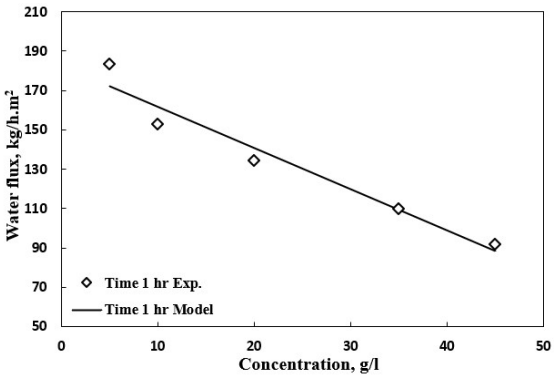

Fig. 9. Experimental and predicted water flux for different feed concentrations.

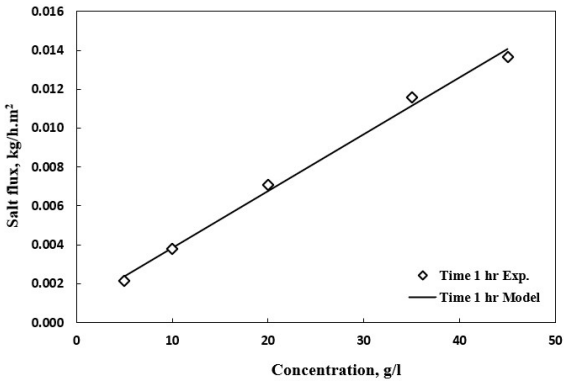

Fig. 10. Experimental and predicted salt flux for different concentrations.

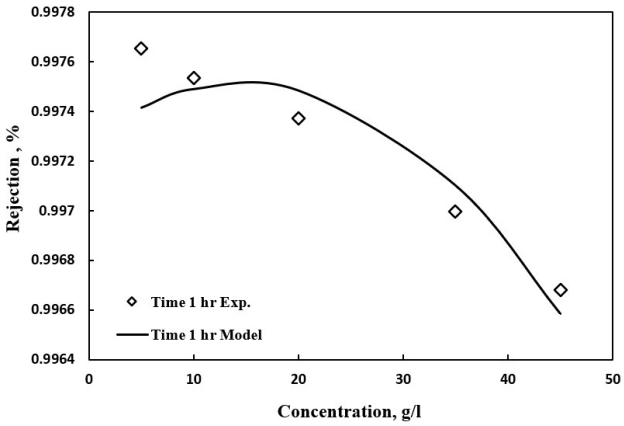

Fig. 11. Comparison between experimental and predicted rejection ratio for different concentrations.

Conflict of Interest

The authors declare that they have no conflict of interest.

References

[1] H. Li, B. Zhu, Y. Feng, S. Wang, S. Zhang, W. Huang, "Synthesis, characterization of TiO_2 nanotubes supported and their photocatalytic activity", J. Solid State Chem., 180 (2007): 2136–2142, DOI: 10.1016/J.JSSC.2007.05.013.

[2] Y. Li, W. Ding, X. Jin, J. Yu, X. Hu, Y. Huang, "Toward extensive application of Pd/ceramic membranes for hydrogen separation: A case study on membrane recycling and reuse in the fabrication of new membranes", Int. J. Hydrogen Energy, 40 (2015): 3528–3537, DOI: 10.1016/j.ijhydene.2014.09.017.

[3] H. Abdallah, R. Taman, D. Elgayar, H. Farag, "Antibacterial blend polyvinylidene fluoride/polyethyleneimine membranes for salty oil emulsion separation", European Polymer J., 108 (2018): 542–553, DOI: 10.1016/j.eurpolymj.2018.09.035.

[4] J. Fang, G. Qin, W. Wei, X. Zhao, L. Jiang, "Elaboration of new ceramic membrane from spherical fly ash for microfiltration of rigid particle suspension and oil–in–water emulsion", Desalination, 311 (2013): 113–126, DOI: 10.1016/j.desal.2012.11.008.

[5] A.A. Gaber, D.M. Ibrahim, F.F. Abd–AImohsen, E.M. El–Zanati, "Synthesis of alumina, titania, and alumina–titania hydrophobic membranes via sol-gel polymeric route", J. Anal. Sci. Technol., 4 (2013): 1–20, DOI: 10.1186/2093-3371-4-18.

[6] B.K. Nandi, R. Uppaluri, M.K. Purkait, "Preparation and characterization of low-cost ceramic membranes for microfiltration applications", Appl. Clay Sci., 42 (2008): 102–110, DOI: 10.1016/j.clay.2007.12.00.

[7] A. Larbot, L. Gazagnesa, S. Krajewskib, M. Bukowska, W. Kujawski, "Water desalination using ceramic membrane distillation", Desalination, 168 (2004): 367–372, DOI: 10.1016/j.desal.2004.07.021.

[8] Z. Cui, W. Peng, Y. Fan, W. Xing, "Effect of cross-flow velocity on the critical flux of ceramic membrane filtration as a pre-treatment for seawater desalination", Chin. J. Chem. Eng., 21 (2013): 341–347, DOI: 10.1016/S1004-9541(13)60470-X.

[9] S. Sobana, and R. Panda, "Review on modelling and control of desalination system using reverse osmosis", Rev. Environ. Sci. Biotechnol., 10 (2011): 139–150, DOI: 10.1007/s11157-011-9233-z.

[10] H. Mehdizadeh, "Modeling of transport phenomena in reverse osmosis membranes", Doctor of Philosophy, McMaster University, CANADA, (1990), https://macsphere.mcmaster.ca/bitstream/11375/6558/1/fulltext.pdf.

[11] S. Sourirajan and T. Matsuura, "Reverse osmosis/ultrafiltration process principles", National Research Council Canada: Ottawa, Canada, (1985).

[12] A. El-Gendi, H. Abdallah, A. Amin, Sh.K. Amin, "Investigation of polyvinyl chloride and cellulose acetate blend membranes for desalination", J. Mol. Struct., 1146 (2017): 14–22, DOI: 10.1016/j.molstruc.2017.05.122.

[13] A. El-Gendi, H. Abdallah, A. Amin, "Economic study for blend membrane production", Bull. Nat. Res. Cent., 45 (2021): 126, DOI: 10.1186/s42269-021-00584-0.

[14] M. Soltanieh, W.N. Gill, "Review of reverse osmosis membranes and transport models", Chem. Eng. Commun., 12 (1981): 279–363, DOI: 10.1080/00986448108910843.

[15] M.A. Mazid, "Mechanisms of transport through reverse osmosis membranes", Sep. Sci. Technol., 19 (1984): 357–373, DOI: 10.1080/01496398408060657.

[16] H.G. Burghoff, K. Lee, W. Pusch, "Characterization of transport across cellulose acetate membranes in the presence of strong solute membrane interactions", J. Appl. Polym. Sci., 25 (1980): 323–347, DOI: 10.1002/app.1980.070250301.

[17] S. Sourirajan, Reverse osmosis. Academic Press, New York, 1970..

[18] A. Alexiadis, D.E. Wiley, A. Vishnoi, R.H.K. Lee, D.F. Fletcher, J. Bao, "CFD modelling of reverse osmosis membrane flow and validation with experimental results", Desalination, 217 (2007): 242–250, DOI: 10.1016/j.desal.2007.02.014.

[19] Y-Z. Liang, K-T Fang, Qing-song Xu, "Uniform design and its applications in chemistry and chemical engineering", Chemom. Intell. Lab. Syst., 58 (2001): 43–57, DOI: 10.1016/S0169-7439(01)00139-3.

[20] Sh.K. Amin, H. Abdallah, S.S. Ali, A.A. Alanezi, "Nano–filtration composite polymeric / ceramic membranes prepared from powder waste of ceramic tile kiln remnants", Desalin. Water Treat., 126 (2018): 67–72, DOI: 10.5004/dwt.2018.23025.

[21] H.H. Abo-Almaged, A.F. Moustafa, A.M. Ismail, Sh.K. Amin, M.F. Abadir, "Hydrothermal treatment management of high alumina waste for the synthesis of nanomaterials with new morphologies", Interceram, 66 (2017): 172–179, https://link.springer.com/content/pdf/10.1007/BF03401212.pdf.

[22] H. Abdallah, A. El-Gendi, M.S. Shalaby, A. Amin, M. El- Bayoumi, A.M. Shaban, "Influence of cellulose acetate polymer proportion on the fabrication of polyvinylchloride reverse osmosis blend membrane, experimental design", Desalin. Water Treat., 116 (2018): 29–38, DOI: 10.5004/dwt.2018.22306.

[23] E. El Zanati, and H. Abdallah, "Esterification of ethyl hexanoic acid using flow-through catalytic membrane reactor", Catal. Ind., 7 (2015): 91–97, DOI: 10.1134/S2070050415020038.

[24] Sh.K. Amin, M.H. Roushdy, S.A. El-Sherbiny, H.A.M. Abdallah, M.F. Abadir, "Preparation of nano–size ceramic membrane from industrial waste", Int. J. Appl. Eng. Res., 11 (2016): 7176–7181.

[25] Sh.K. Amin., H.A.M. Abdallah, M.H. Roushdy, S.A. El-Sherbiny, "an overview of production and development of ceramic membranes", Int. J. Appl. Eng. Res., 11 (2016): 7708–7721.

[26] H. Abdallah, Sh.K. Amin, H.H. Abo-Almaged, M.F. Abadir, "Fabrication of ceramic membranes from nano–rosette structure high alumina roller kiln waste powder for desalination application", Ceram. Int., 44 (2018): 8612–8622, DOI: 10.1016/j.ceramint.2018.02.077.

[27] Sh.K. Amin, M.H. Roushdy, H.A.M. Abdallah, A.F. Moustafa, M.F. Abadir. "Preparation and characterization of ceramic nanofiltration membrane prepared from hazardous industrial waste", Int. J. Appl. Ceram. Technol., 17 (2020): 162–174, DOI: 10.1111/ijac.13311.

[28] S. Emani, R. Uppaluri, M.K. Purkait, "Preparation and characterization of low-cost ceramic membranes for mosambi juice clarification", Desalination, 317 (2013): 32–40, DOI: 10.1016/j.desal.2013.02.024.

[29] Y.A.W. Shardt, "Statistics for chemical and process engineers – A modern approach", 1st Edition, Springer International Publishing, Switzerland, (2015), ISBN: 978-3-319-38749-9, DOI 10.1007/978-3-319-21509-9

[30] Sh.K. Amin, H.A.M. Abdallah, A.M. Ismail, A. El-Gendi, S.A. El-Sherbiny, "Economic study for Green Nano-ceramic Membrane Production", Egypt. J. Chem., Available online, (2021), DOI: 10.21608/ejchem.2021.94795.4532.

[31] D. Rashad, Sh.K. Amin, M.S. Mansour, H. Abdallah, "Fabrication of low-cost antibacterial microfiltration tubular ceramic membranes", Ceram. Int., Available online, (2022), DOI: 10.1016/j.ceramint.2022.01.005.

[32] D. Rashad, Sh. K. Amin, M.S. Mansour, H. Abdallah, "A systematic literature review of ceramic membranes applications in water treatment", Egypt. J. Chem., Available online, (2022), DOI: 10.21608/ejchem.2021.105802.4871.

[33] D. Ewis, N.A. Ismail, M.A. Hafiz, A. Benamor, A.H. Hawari, "Nanoparticles functionalized ceramic membranes: fabrication, surface modification, and performance", Environ. Sci. Poll. Res., 28 (2021): 12256–12281, DOI: 10.1007/s11356-020-11847-0.

[34] S.A. El-Mekkawi, N.N. El-Ibiari, O.A. El-Ardy, N.M. Abdelmonem, A.H. Elahwany, M.F. Abadir, I.M. Ismail, "Optimization of cultivation conditions for Microcystis aeruginosa for biodiesel production using response surface methodology", Bull. Nat. Res. Cent., 44 (2020): 6, DOI: 10.1186/s42269-019-0265-9.